Structure of the Topoisomerase IV C-terminal Domain from *Bacillus stearothermophilus*

Bacteria possess two closely related yet functionally distinct essential type IIA topoisomerases (Topos). DNA gyrase supports replication and transcription with its unique supercoiling activity, whereas Topo IV preferentially relaxes (+) supercoils and is a decatenating enzyme required for chromosome segregation. Here we report the crystal structure of the C-terminal domain of Topo IV ParC subunit (ParC-CTD) from Bacillus stearothermophilus and provide a structure-based explanation for how Topo IV and DNA gyrase execute distinct activities. Although the topological connectivity of ParC-CTD is similar to the recently determined CTD structure of DNA gyrase GyrA subunit (GyrA-CTD), ParC-CTD surprisingly folds as a previously unseen broken form of six-bladed β-propeller. Propeller breakage is due to the absence of a DNA gyrase-specific GyrA box motif, resulting in the reduction of curvature of the proposed DNA binding region, which explains why ParC-CTD is less efficient than GyrA-CTD in mediating DNA-bending, a difference leads to divergent activities of the two homologous enzymes. Moreover, we found that the topology of the propeller blades observed in ParC-CTD and GyrA-CTD can be achieved from a concerted β-hairpin invasion-induced fold change event of a canonical six-bladed β-propeller; hence we proposed to name this new fold as "hairpin-invaded β-propeller" to highlight the high degree of similarity and a potential evolutionary linkage between them. The possible role of ParC-CTD as a geometry facilitator during various catalytic events and the evolutionary relationships between prokaryotic type IIA Topos have also been discussed according to these new structural insights.

In bacteria, the resolution of DNA entanglements and maintenance of topological homeostasis are largely handled by two essential type IIA topoisomerases (Topos), DNA gyrase and Topo IV. Interestingly, although DNA gyrase and Topo IV share a high degree of similarity, they possess distinct cellular functions and thus cannot complement each other *in vivo*. DNA gyrase is the only type IIA enzyme capable of actively introducing (-) supercoils into DNA, an activity involved in replication initiation and transcription of (-) supercoil-dependent promoters. In contrast, Topo IV does not possess supercoiling activity and is normally localized behind the replication forks to serve as a decatenating enzyme for disentangling the interlinked daughter chromosomes.

In addition to its apparent function in decatena-tion, *in vitro* analyses also revealed that Topo IV is able to catalyze relaxation of supercoiled DNA. Recent studies show that Topo IV relaxes (+) supercoils much faster than (-) supercoils. By engaging single-molecule relaxation assays on mechanically braided DNA molecules, Cozzarelli and Charvin's groups hypothesized that Topo IV is able to sense the geometry of DNA crossovers; a left-handed crossing of the T- and G-segments imposed by the (+) superhelix makes a preferred substrate for duplex passage reaction.

How do homologous type IIA Topos diverge in catalytic activities and substrate specificities? Detailed sequence comparison predicted that the C-terminal domains (CTDs) of both DNA gyrase (GyrA-CTD) and Topo IV (ParC-CTD) may adopt a six-bladed β-propeller fold. Deletion analysis further established that the negative supercoiling activity of DNA gyrase is dependent on GyrA-CTD. Given the functional significance of this domain, it is likely that the differences between DNA gyrase and Topo IV can be attributed in part to their respective CTDs. To provide a structural basis for their functional differences and to understand the catalytic role of this domain, we have determined the crystal structure of ParC-CTD.

ParC-CTD is composed of six highly-twisted antiparallel β-sheet modules arranged sequentially along a curved surface to give an overall arc-shaped appearance (Fig. 1A). This architecture approximates the well-known β-propeller structures and resembles the newly discovered GyrA-CTD β-pinwheel in particular. However, in sharp contrast to other β-propeller structures (including GyrA-CTD β-pinwheel) where the first and the last propeller blades are always tethered together to form a closed-ring structure, a gap is clearly present in the ParC-CTD between blades 1 and 6, resulting in breakage of the six-bladed β-propeller ring (Fig. 1A). To our knowledge, ParC-CTD reveals for the first time that a protein can fold as a broken β-propeller without ring-closure.

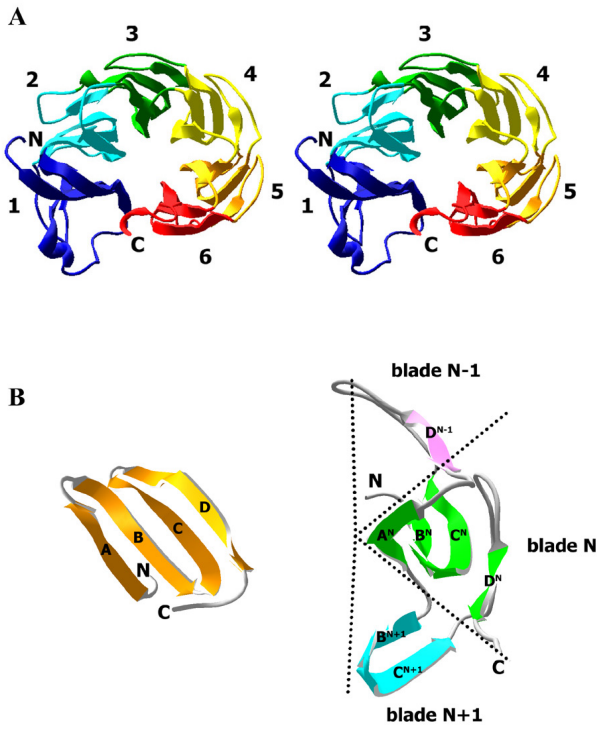

Fig. 1: A) Stereo ribbon representation of the ParC-CTD from B. stearothermophilus viewed along the central propeller shaft. Blades 1-6 are numbered along the sequence and colored individually. B) Comparison of the strand connectivity between a canonical -propeller blade (left) with the novel "hairpin-invaded" propeller blades of ParC-CTD (right) in ribbon diagram. The four -strands (A-D) of each ParC-CTD blade are named according to their spatial order following the nomenclature used for canonical -propeller structures. The superscriptions N-1, N, and N+1 are used to distinguish strands of different blades.

Another prominent feature of ParC-CTD resides in the complex topology of its propeller blades (Fig. 1B). This novel folding pattern was first observed in the GyrA-CTD β-pinwheel, and an unusual type of four-stranded repeating unit that conforms to the Greek key connectivity was defined by Corbett *et al*. to highlight the overall pinwheel topology. However, to be consistent with the nomenclature used to describe the canonical β-propeller structures, we feel that a single β-sheet in GyrA-CTD and ParC-CTD should be used to define a propeller blade. We suggest that the type of β-sheets observed in GyrA-CTD and ParC-CTD can be referred to as "hairpin-invaded β-propeller blades" (Fig. 1B). Since invasion of a β-strand(s) into existing β-sheets has been viewed as a common mechanism for triggering fold change, it is reasonable to hypothesize that ParC-CTD of *B. stearothermophilus* may have evolved from an ancestral six-bladed β-propeller structure via a concerted β-hairpin invasion-mediated fold change event.

Recent results obtained from FRET experiments indicated that both GyrA-CTD and ParC-CTD are capable of bending DNA, despite the former one being more effective. It was proposed based on this finding that ParC-CTD may facilitate the recognition and positioning of T-segment DNA. To understand how ParC-CTD may interact and bend DNA, its surface electrostatic features were examined. A continuous electropositive patch about 25 Å wide and 95 Å in length was identified on the outer surface of ParC-CTD, suggesting a potential binding region for double-stranded DNA (Fig. 2A). The dimension and curvature of this positively charged region appeared suitable for bending DNA because a 36 bp of curved duplex DNA taken directly from the nucleosome core particle can fit nicely along this surface in an *in silico* docking analysis (Fig. 2B). In line with its potential functional significance, analysis of conserved surface residues reveals that this prospective DNA-binding region is comprised of highly conserved residues (Fig. 2C).

A major functional difference between ParC-CTD and GyrA-CTD is that the latter is more effective in introducing DNA bending (30). The structure of ParC-CTD provides two indications that suggest why GyrA-CTD bends DNA more efficiently. The most prominent difference betweenthe two is that ParC-CTD does not fold as a closed-ring structure as GyrA-CTD (Fig. 3A). The proposed DNA-binding region of GyrA-CTD therefore has a steeper surface curvature than that of ParC-CTD, which may account for their different bending efficiency. If such a structure/function relationship does exist, then the functional significance of a conserved DNA gyrase-specific short amino-acid sequence, termed GyrA box, can be readily inferred.

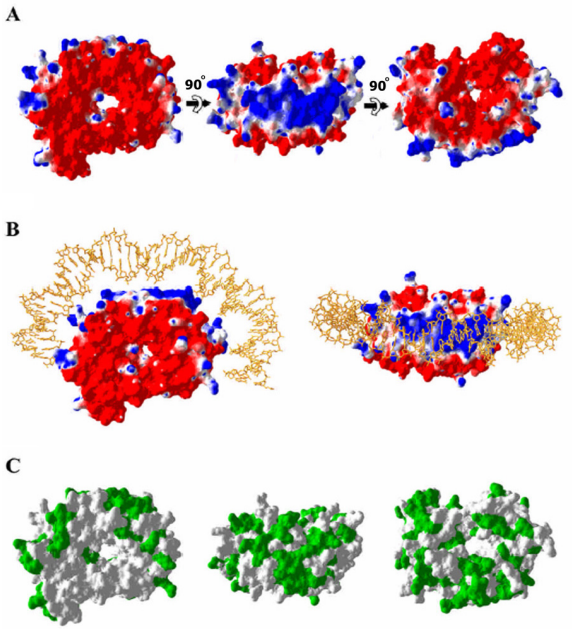

Fig. 2: A) Electrostatic surface representation of ParC-CTD. Basic, acidic, and uncharged surface regions were colored blue, red, and white, respectively. B) Model for a 36 bp DNA fragment binding to the electropositive outer perimeter of ParC-CTD. C) Surface representation of conserved residues in ParC-CTDs of Gram positive bacteria.

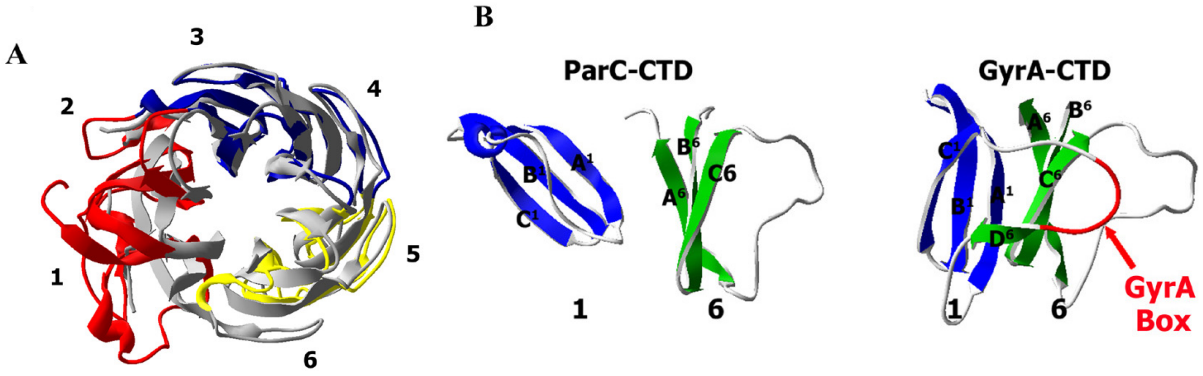

Fig. 3: A) Ribbon diagram showing the superimposition of ParC-CTD and GyrA-CTD. GyrA-CTD is shown in grey. B) Views of blades 1 (blue) and 6 (green) in ParC-CTD and GyrA-CTD. The GyrA box motif that packs against strand C6 and mediates ring-closure in GyrA=CTD is highlighted in red.

For GyrA-CTD, ring closure was mediated mainly by the strand exchange between blades 1 and 6 in which the loop follows strand C^1 wraps and packs against the strand C^6 (Fig. 3B). Because GyrA box (highlighted in red in Fig. 3B) resides in the middle of this loop and makes extensive interactions with the core residues of blade 6, it is reasonable to expect that the closed-ring structure of GyrA-CTD would be significantly destabilized when the GyrA box is missing, resulting in a broken β-propeller as observed in ParC-CTD. Our analysis supports the use of GyrA box as a key determinant in the functional annotation of newly sequenced bacterial genomes.

Finally, based on the unique substrate specificity of Topo IV and the apparent DNA-binding capability of its CTD, we proposed the following models to illustrate how ParC-CTD might affect various reactions catalyzed by Topo IV (Fig. 4). During the relaxation of (+) supercoiled substrate, the T-segment is placed at a left-handed crossover position suitable for rapid duplex passage reaction (Fig. 4A). Although ParC-CTD interacts with the T-segment DNA in this case, this domain is likely to be dispensable for relaxation because the catalytic productive crossover is already imposed by the (+) superhelix. Higher (+) σ accelerates relaxation by facilitating the formation of such a DNA crossing geometry. In contrast, by favoring a right-handed crossover, (-) supercoiled DNA is usually a poor substrate for relaxation (Fig. 4B-1). However, the non-productive binding mode can be converted into a catalytic proficient left-handed node with the help of ParC-CTD (Fig. 4B-2), and the slower relaxation rate is likely due to the requirement for this additional step. Negative σ values discourage relaxation by inhibiting this essential conformational change of DNA. Similarly, ParC-CTD may facilitate decatenation by positioning the T- and G-segments into a preferred orientation for duplex passage reaction (Fig. 4C). Taken together, we suspect ParC-CTD plays different roles during Topo IV catalysis.

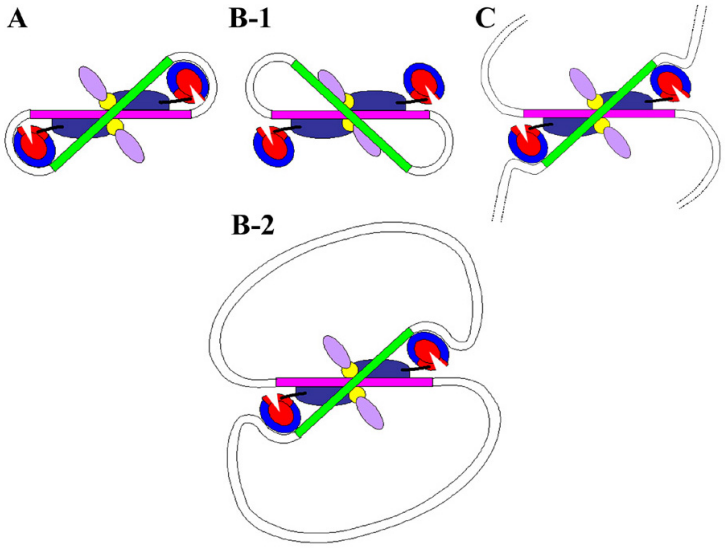

Fig. 4: Proposed geometry facilitator role of CTD during various Topo IV-catalyzed reactions: A) relaxation of (+) supercoils, B-1) non-productive binding mode for relaxation of (-) supercoils, B-2) productive binding mode for relaxation of (-) supercoils, and C) decatenation.

In conclusion, we have determined the crystal structure of ParC-CTD from *B. stearothermophilus* to 1.8 Å resolution using the Se-MAD approach. Although ParC-CTD displays similar topological connectivity as observed in GyrA-CTD, profound differences have been identified. ParC-CTD folds as a broken form of six-bladed β-propeller, and this breakage or non-closure in the propeller structure is due to the absence of a DNA gyrase-specific GyrA box motif. As a result, the curvature of the proposed DNA binding region in ParC-CTD is reduced and the DNA bending capability of this domain is less efficient. These differences provide a structural explanation as to why Topo IV and DNA gyrase execute divergent activities and how ParC-CTD is involved in positioning the DNA duplexes for catalysis.

BEAMLINE
SP12B2 Protein X-ray Crystallography beamline
17B2 W20 Protein Crystallography beamline

EXPERIMENTAL STATION
Protein Crystallography end station

AUTHORS
T.-J. Hsieh and N.-L. Chan
Institute of Biochemistry, National Chung Hsing University, Taichung, Taiwan

L. Farh
Department of Natural Science Education, National Pingtung Teachers College, Pingtung, Taiwan

W. M. Huang
Department of Pathology, University of Utah, Salt Lake City, USA

PUBLICATIONS
- T.-J. Hsieh, L. Farh, W. M. Huang, and N.-L. Chan, J. Biol. Chem. **279**, 55587 (2004).

CONTACT E-MAIL
nlchan@dragon.nchu.edu.tw